RSC Advances

This is an *Accepted Manuscript*, which has been through the Royal Society of Chemistry peer review process and has been accepted for publication.

Accepted Manuscripts are published online shortly after acceptance, before technical editing, formatting and proof reading. Using this free service, authors can make their results available to the community, in citable form, before we publish the edited article. This *Accepted Manuscript* will be replaced by the edited, formatted and paginated article as soon as this is available.

You can find more information about *Accepted Manuscripts* in the Information for Authors.

Please note that technical editing may introduce minor changes to the text and/or graphics, which may alter content. The journal's standard Terms & Conditions and the Ethical guidelines still apply. In no event shall the Royal Society of Chemistry be held responsible for any errors or omissions in this *Accepted Manuscript* or any consequences arising from the use of any information it contains.

ROYAL SOCIETY OF CHEMISTRY

www.rsc.org/advances

Understanding integrated effects of humidity and interfacial transfer films formation on tribological behaviors of sintered polycrystalline diamond

Wenbo Qin[a], Wen Yue[a, b*], Chengbiao Wang[a, b]

a. School of Engineering and Technology, China University of Geosciences (Beijing), Beijing 100083, PR China.

b. Key Laboratory on Deep Geo-drilling Technology of the Ministry of Land and Resources, China University of Geosciences (Beijing), Beijing 100083, PR China.

W.B. Qin. E-mail address: wbq8008@163.com, Tel.:13269678008

Corresponding Author: *W. Yue. E-mail address: cugbyw@163.com, yw@cugb.edu.cn.

Tel.:+086 10 82320255. Fax: +086 10 82322624.

RSC Advances Accepted Manuscript

Abstract: Polycrystalline diamond (PCD) used in down-hole tool applications is ideally suit for harsh environments such as drilling at circulation break and poor lubrication, in which the water molecules of physical and chemical adsorption can severely affect the tribochemistry effect across cutting interface. Here, tribological behaviors of PCD are studied in a controlled humid atmosphere (5%-50% RH). The friction coefficient is ~ 0.04 under 5% RH condition, which is significantly increased to ~ 0.11 under 50% condition. The run-in period and wear rate of PCD decrease while increasing RH levels during the tribotest. Such an ultra-low friction coefficient regime is explained coincide with the formation of efficient carbonaceous transfer films in the run-in periods through *ex situ,* micro-laser Raman spectroscopy and Atomic Force Microscope (AFM) measurements.

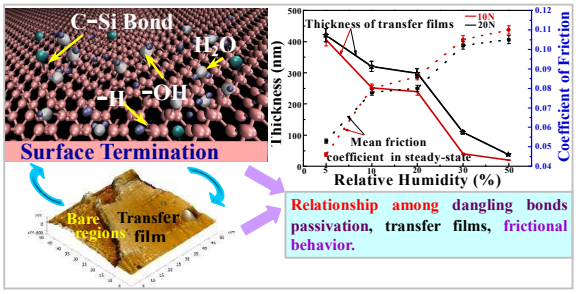

Abstract graph: This paper highlights an intimate relationship among RH levels, dangling bonds passivation, run-in periods, transfer films formation and tribological behaviors.

1. Introduction

Sintered polycrystalline diamond (PCD) prepared by high pressure and high temperature (HP/HT) has been widely used in machining tools, thrust bearings and drill

RSC Advances Accepted Manuscript

bits due to its extremely high wear resistance, high hardness and excellent toughness. Among these applications, fluids such as water, drilling mud and gas, are always required to lubricate the surfaces and interfaces of PCD in down-hole applications and its counter frictional pair.[1-4] Previous works have focused on that diamond rubbing against diamond in the presence of oil and water based drilling fluids had a coefficient of friction between 0.05 and 0.08.[5] Sexton *et al*.[6] investigated the bearing wear rates in laboratory testing and results showed that PCD thrust bearings provide a long-lasting bearing solution for down-hole drilling tools. Knuteson *et al*.[7] reported that the friction coefficient values of PCD thrusting bearing decreased in the lubrication regime moving from boundary to mixed-mode and may even become hydrodynamic. Mehan *et al*.[8] measured the wear rates of PCD and pointed out that wear mechanism of PCD was the result of diamond particles falling off in pin-on-disk tribometer experiments. However, the above works only concentrated on the mechanical aspects of wear performance and have not addressed the role of service environment factors on the friction coefficient, wear and ultimate failure wear of PCD. Considering the operating conditions such as high speeds, high loads, run-in period, frequent starting and stopping, cyclic fluctuating loads and extreme conditions such as drilling at circulation break and poor lubrication, the PCD contact surfaces cannot be ensured keeping in liquid lubrication condition all the time. We have confirmed from tribological behaviors of PCD under different relative humidity (RH) that friction coefficient, wear and adhesion behaviors are significantly affected by the adsorbed water molecules which can have distinct impacts on physical and chemical properties of solid surfaces. Understanding the effects of the relative humidity on sliding interface would be

RSC Advances Accepted Manuscript

beneficial to achieve lower friction and wear, and longer service life for PCD tools.

Many well-known experimental and simulated researches have been proposed to illustrate the effects of environmental humidity on the tribological behaviors of diamond materials. It is shown that friction coefficient and wear are strongly influenced by the humidity levels during the tribotest. Enke *et al*.[9] have demonstrated that humidity have a strong effect on the friction coefficient of diamond-like carbon (DLC) film, the friction coefficient of DLC can keep in 0.01-0.02 under a low RH<1% testing environment, however, the friction coefficient rapidly rise to ~ 0.2 at 100% RH. This is similar to the report published by Marino *et al*.[10] Konicek *et al*.[11] also reported that the ultralow friction and wear of ultrananocrystalline diamond (UNCD) originate from the H_2O dissociative passivation of surface dangling bonds during sliding. Analogously, Kumar *et al* [12] studied the tribotest at low load in ultra-nanocrystalline diamond film shows increase in friction coefficient with decrease in RH value. Recently, Zhao *et al*.[13] reported the friction coefficients of the PCD sliding against silicon nitride (Si_3N_4) spheres under vacuum are ~ 1.1, which is ten times higher than ~ 0.11 that under ambient air. Such a distinct frictional performance immediately demonstrated the effects of a passivated surface with the absorbed species on decreasing adhension interaction across the sliding interface.

The tribological behaviors of diamond materials are still influenced by the formation of transfer film at sliding interface.[14] Many investigations have demonstrated that the formation of carbonaceous transfer layer on sliding ceramic counterbodies often influences tribological properties of diamond materials.[15-18] It has also been speculated that the low friction after run-in period of polycrystalline diamond films is due to the

RSC Advances Accepted Manuscript

formation of a transfer layer, possibly graphitic in nature.[19] Transfer films are known to play an important role in the friction of dry sliding contacts. Chen *et al*.[20] have reported that the rapid buildup of running-in-induced friction reducing tribolayers at the contact interface, which is more feasible in self-mated in a‑C:H:Si films sliding, and the tribolayers can be crucial for achieving a superlubric state. In contrast, Radhika *et al*.[21] has recently reported the role of transfer films on tribological properties of nanocrystalline diamond nanowire film sliding against alumina allotropes. A carbonaceous transfer layer was formed on sapphire and ruby balls with friction coefficient values ~0.06 and ~0.07, comparing with aluminum oxide (Al_2O_3) ball without transfer layer formed with super low friction coefficient ~0.003. They pointed out the reason is that sliding occurs between film and the carbonaceous transfer layer formed on the ball exhibiting high energy due to covalent carbon bonds which chemically interact and enhance sliding resistance. It can not be ignored as the symbiosis phenomenon that can seriously influence the tribological performance of amorphous or nanocrystalline diamond materials.[22] However, up to now, little attention has been paid to the prominent role between water molecule adsorption and the transfer films formation during frictional sliding on PCD surfaces.

Three main hypotheses have been proposed to explain the tribological behaviors of relative diamond materials. The first one, experimental and theoretical studies have highlighted the beneficial effect of dangling bonds passivation theory by forming H-terminated, OH-terminated and other species-terminated surface at sliding interface on the tribological performance of such carbon films.[11,23-26] These un-saturate dangling bonds on the topmost surface of carbon-based materials are with high surface energies, which

RSC Advances Accepted Manuscript

can form covalent interaction.[27] Diamond surfaces saturated by the dissociative adsorption of water molecule can decrease the adhesion interaction at the sliding interface supported by ab initio density functional theory (DFT) calculations and molecular dynamics simulations.[28]

Next one, according to Tabor's adhesion theory,[29] the frictional force provides the energy to break the bonds formed at the interface of contact between the carbon atoms from the two surfaces. Due to the large amounts of dangling bonds which are not saturated by adsorbed species in vacuum, the adhesion theory successfully explains the frictional mechanism of diamond sliding on diamond in vacuum exhibiting higher friction coefficient value (0.5-1 compared to values between 0.05-0.15 in air) by forming intense adhesive.[13,30]

Moreover, a theory carbon rehybridization ($sp^3 \rightarrow sp^2$ conversion) can take place at sliding interface.[11,14,31] Several studies found that diamond materials with increased sp^2 fractions exhibit lower friction and wear by making films more lubricious.[18,32] Amorphous carbon-based films with more sp^2 content have a shear-induced carbon phase transformation process such as the conversion from sp^3- to sp^2-bonded carbon at the sliding interface with the detection of D-peaks (~1360 cm^{-1}) and G-peaks (~1585 cm^{-1}) by Laser Raman spectroscopy.[14,17,19,33-34] The sp^2-C phase is thought to be a softer and low-shear strength phase corresponding to the possible formation of a carbonaceous tribolayer at the sliding interface.[21,35]

The relative humidity in the testing environment plays a crucial role on the tribolobical properties of diamond materials. However, a carefully measurement and

RSC Advances Accepted Manuscript

systematic investigation of the effect of relative humidity levels and transfer films formation on the tribological behaviors of sintered PCD have not been reported. In this work, for the first time, we examined the run-in and steady-state behaviors of PCD by varying the normal load and relative humidity levels to gain insight into the mechanism of transfer films formation that govern friction and wear for the tribologically exceptional PCD materials.

2 Experimental details

2.1 Fundamental characteristics of specimens

Polycrystalline diamond compact (PDC) is usually applied to down-hole drilling tools such as thrusting bearing and drilling bits. The PDC is composed of the top PCD layer and the tungsten carbide substrate with cobalt binder (WC-Co). PDC specimens are sintered at Zhongnan Diamond Co., Ltd. using a high pressure and high temperature (HP/HT) technique. The PDC is consisted of a WC-16 wt. % Co cemented carbides substrate with a PCD layer sintered onto the circular surface of the substrate. Its dimensions are approximately 45 mm in diameter and 2.9 mm in thickness of PCD layer. PCD layer is composed of a coarse grain (half-content diameter, D50 = 25 μm) diamond with Co binder and a surface roughness (Ra) ~ 3-4 nm (It is measured by the Atomic Force Microscope). Fig. 1 displayed the fundamental characteristic of PDC. Furthermore, a Si_3N_4 sphere was selected as a counterpart in tribotests. Its diameter is 4 mm and roughness (Ra) is 15-20 nm. The main physical properties of the PCD and the Si_3N_4 sphere are listed in Table 1.

RSC Advances Accepted Manuscript

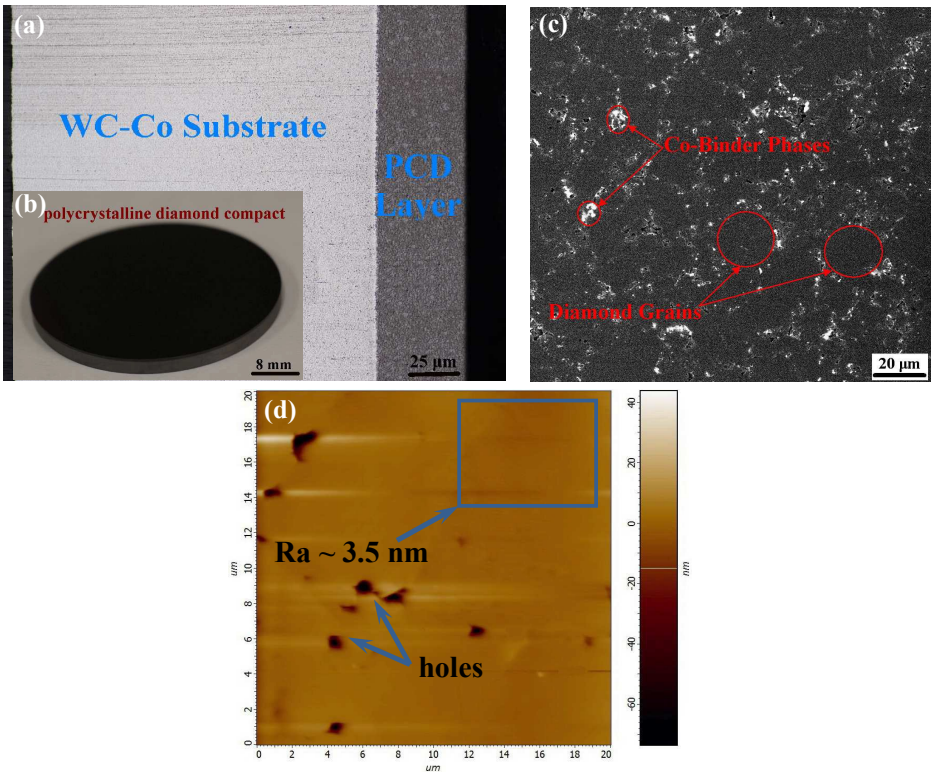

Fig. 1 The characteristics of PDC: (a) cross-sectional image, (b) profile of PDC, (c) back scattering morphology of PDC's surface and (d) AFM topography of the PCD surface.

2.2 Ball-on-disc tribotests

The tribotests were performed on a MS-T3000 type ball-on-disc rotation tribometer housed inside an environmentally controlled chamber using to measure friction coefficient (schematics as shown in Fig. 2). The lateral force exerted to the sphere during the sliding process was measured with a strain gauge sensor and the friction coefficient was calculated by Amonton's law.[36] Humidity levels were introduced by controlling the flow of dry nitrogen through a breaker containing deionized water, the relative humidity of tribometry chamber can be accessibility controlled from ~ 5% RH to ~ 95% RH. Relative humidity measured with hygrometer (Londi Sun LS-207 Type), which is accurate within ± 0.1%, with a lower detection limitation of 5%.

RSC Advances Accepted Manuscript

The influence of loads and RH levels on the tribological behaviors of PCD was measured. The drilling bits surface always service under extreme environments such as alternate loads and non-fluid lubrication conditions (e.g., jamming of the drilling bits results in humid service conditions). Two applied normal load of 10 N and 20 N were fixed, and six levels of RH (5%, 7%, 10%, 20%, 30%, and 50%) were used. According to the calculation of Hertzian theory, the initial mean Hertzian contact pressure is 1.86 GPa and 2.39 GPa for 10 N and 20 N, respectively. The PCD specimen was fixed on a rotary sample platform using a Si_3N_4 sphere as a counterpart with the rotation radius of 5 mm and rotation speed of 400 rpm corresponding to drill bits drilling liner velocity ~ 215-940 rpm.[37] In order to guarantee the steady values of RH in testing chamber, the RH reaches the specified value and stabilizing for 15 minutes before the tribotests. Prior the tribotest, both the sphere and PDC samples were rinsed with acetone for 30 minutes, and then ultrasonically cleaned in alcohol for 30 minutes. After tribotests both the spheres and PDC samples were rinsed with alcohol for 10 minutes. Consequently, each tribotest was performed two times and the data were found to be approximately similar.

2.3 Microanalysis methods

A Nikon optical microscope (Olympus BX51M) was employed to image the morphology of the transfer film formed on the Si_3N_4 spheres. The morphology and topography of the wear tracks were measured by NanoMap-D three-dimensional White Light Interferometer. A Lab RAM HR Evolution Raman spectroscopy (HORIBA Jobin Yvon) (spot diameter of laser is 1.25 μm, Ar^+ laser wavelength is 514.5 nm) was conducted to analyse the wear scars on the Si_3N_4 spheres and wear tracks on the PCD

RSC Advances Accepted Manuscript

surfaces. Atomic Force Microscope-Lateral Force (AFM-LF) (NTEGRA PRIMA) was used to measure the surface structure and topography and friction force in nanoscale of carbonaceous transfer films formed on wear scars. The Point Probe Plus Contact Mode (PPP-CONT) probe with a Si_3N_4 tip was selected to scan the surface of transfer films. The scanning frequency and scope is 1 Hz and 50×50 μm, respectively.

Table1. Physical properties of PCD and Si_3N_4.

Properties	Density (g/cm^3)	Young's modulus (GPa)	Hardness (GPa)	Thermal conductivity (W/(m×K))	Poisson's ratio
PCD	3.3~3.7	810	30~40	700	0.070
Si_3N_4	3.4	260~320	15~20	1.67~2.09	0.250

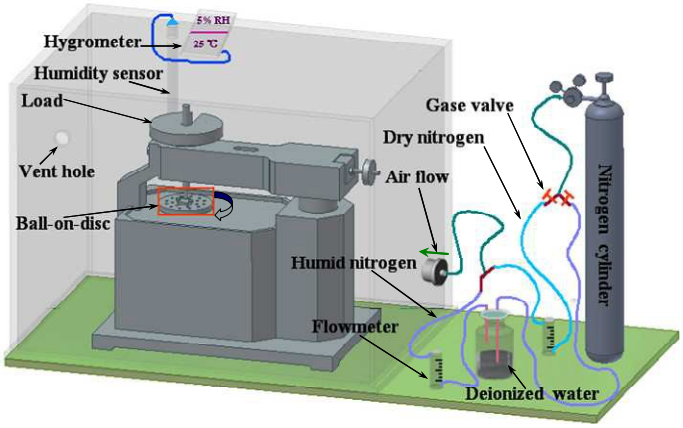

Fig. 2 Schematics of ball-on-disc tribometer and the relative humidity controls system.

3. Results

3.1 Run-in period performance dependent on the RH levels

Understanding the role of the run-in behaviors and the effects of transfer films formation on PCD friction and wear are important to design optimum operation conditions for PCD application and to prevent potential failures of PCD layer. Experimental

RSC Advances Accepted Manuscript

elucidation of the role of humidity with dangling bond passivation theory of the H-terminated, OH-terminated surface and the formation of transfer film on the friction of diamond materials is complicated by the fact that it can be difficult to isolate the influence of these factors on adhesion and friction.[11,16,24,28] The effects of dangling bonds passivation will be described in detail hereinafter.

Run-in behavior is often correlated to the initial interactions between the asperities of two surfaces.[38] This process results in locally high contact stresses that lead to plastic deformation, wear and the creation of third-bodies.[10,39-40] The curve of friction coefficients versus cycle is plotted in Fig. 3a, c. Under 5% and 7% RH conditions, there are similar variation in friction coefficient and run-in periods. In order to more clearly compare the RH dependence of run-in period and steady-state friction coefficient, the effect of RH levels (5%, 10%, 20%, 30% and 50%) on tribological behavior of PCD is mainly analyzed and discussed in this paper. Test performed at 5% RH, it always exhibites an induction period, so-called “run in” period, during which the friction coefficients reach the highest value (the initial maximum friction coefficient ~0.47 for 10 N and ~0.4 for 20 N) and gradually decrease before reaching an low steady-state friction coefficient (~0.04 for 10 N and ~0.06 for 20 N) (Fig. 3a, c). The testing conducted at 10 N, 5% RH within 4000 cycles of run-in period higher than at 20 N, 5% RH within 2000 cycles. Interestingly, the longer run-in period corresponded to the lower steady-state friction coefficient. During the sliding testing, a slight vibration of the ball-on-flat tribo-tester occur in the initial period, at the same time, we heard some intermittent squeak noise. It is likely due to sticking of the slider during the first few small-amplitude cycles, and this phenomenon may be called

RSC Advances Accepted Manuscript

"stick slip". However, when water molecules were introduced into testing environment, the frictional performance in humidity atmosphere is entirely different from the dry conditions 5% RH. In the various RH levels (10% RH-50% RH) environment, the friction coefficients are rapidly reach steady-state with short run-in period occur (Fig. 3b, d) and a decreasing tendency of reaching steady-state with increasing relative humidity. These phenomena exert obviously different in various RH level atmospheres. In other words, for each test that achieved low friction there is an inverse relationship between RH level and number of run-in cycles, and the steady-state friction coefficients slowly increase with the increasing of RH level from 10% to 50%. However, the friction coefficient in the humid environment is higher than that in the dry testing conditions (Fig. 3a, c). Similar to results under 10 N shown in Fig. 3a, a clear negative correlation relationship exists between steady-state friction coefficient and RH levels for 20 N displayed in Fig. 3c.

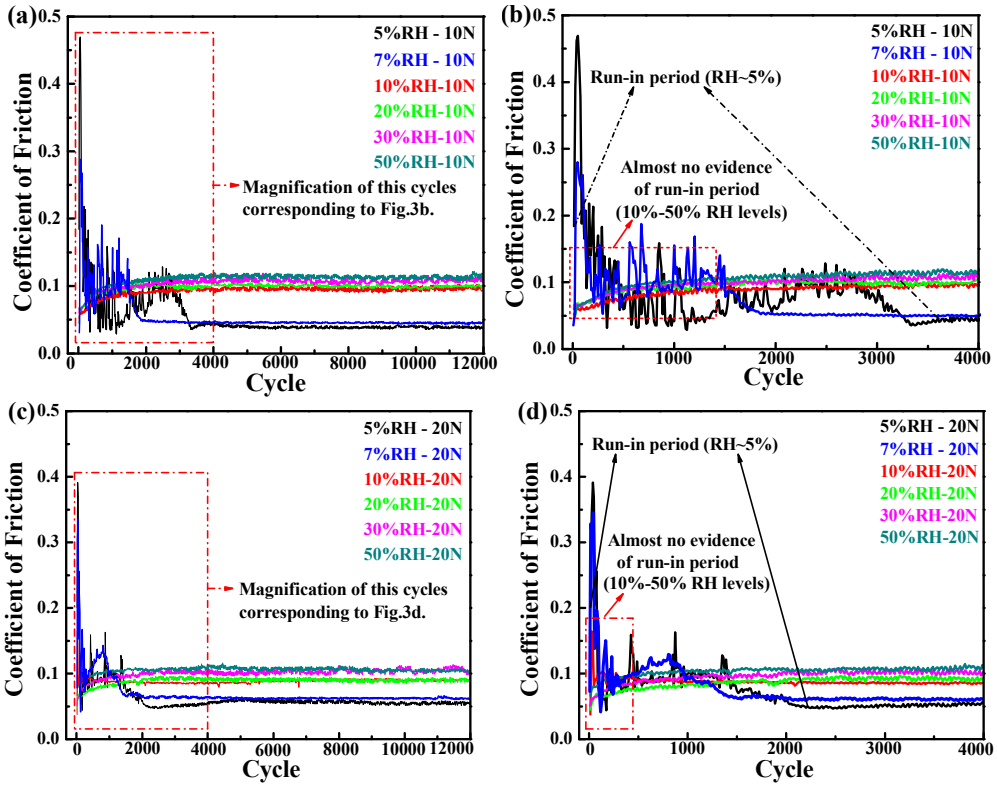

RSC Advances Accepted Manuscript

Fig. 3 Friction coefficients versus cycles for PCD/Si_3N_4 under different RH and loads at room temperature. (a), (c) Friction plot for the total cycles to compare the steady-state friction coefficient. (b), (d) The amplification of the first 4000 cycles depicted with red gitternetzlinien shown in Fig. (a), (c) to highlight the comparison of run-in period at different RH levels.

After the tribotests, there are clearly noticeable contact slide marks on the counter ball surfaces. Fig. 4 shows the optical wear morphologies of sliding pars in the contact area under different RH levels and loads. It is obviously seen that multicolor wear scars, partially (Fig. 4 a1-a4, b1-b4) or barely (Fig. 4 a5, b5) covered by tribo-induced transfer films, formed on the Si_3N_4 spheres with different continuity. From the optical image of wear scar region formed under 5% RH at 10 N and 20 N, these are clearly noticeable integrity transfer films formation corresponding to the ultralow friction coefficient (~0.04 for 10 N and ~0.06 for 20 N described in Fig 3). Due to the amount of water molecules in 5%RH level is not enough, these exert the effect of dangling bonds passivation and then the strong covalent interactions between the unsaturated atoms occurred. These covalent interactions result in bonds broken with the formations of carbonaceous transfer film. However, when the RH level reaches 10%, the water molecules are still enough to have strong dangling bonds passivation effect on preventing the formations of transfer film. In addition, a large amount of transfer film debris is still heaped on the edge of the wear scar regions after cleaning with alcohol. The diameters of wear scars increase with the variation of RH levels from 10% to 50% both for 10 N and 20 N. Due to the strong covalent interaction between PCD un-terminated surfaces and Si_3N_4 spheres at 5% RH condition, a higher wear scar is still formed. It infers that these transfer films are mainly

RSC Advances Accepted Manuscript

transferred from the PCD layer with tribochemical reaction which will be discussed using Raman spectroscopy and AFM measurements below.

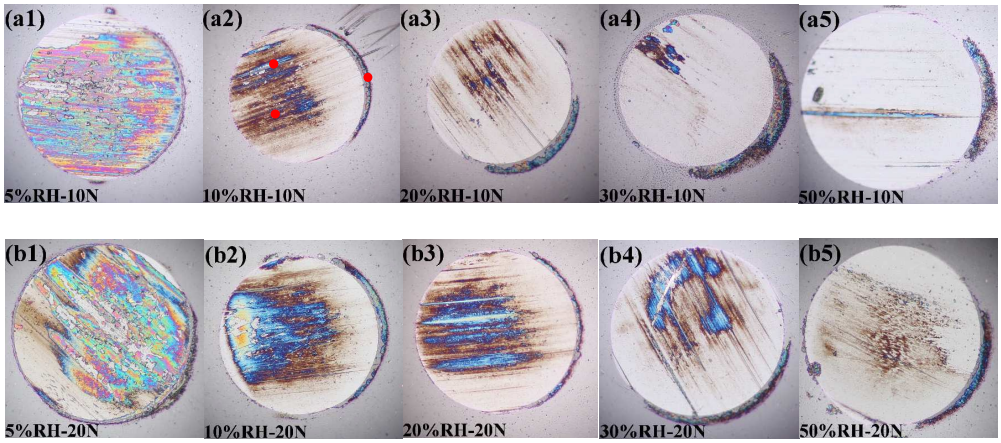

Fig. 4 The optical images of wear morphologies of wear scars formed on the Si_3N_4 spheres after frictional tests in different RH and loads: a1-a5 wear scars formed at load 10 N and b1-b5 at load 20 N. The red dots marked in Fig. indicate the positions for Raman analysis, as will be discussed hereinafter.

The wear tracks on the PCD surfaces are so narrow that it is hard to see but identifiable. This phenomenon is similar to that publised in Marino's study understanding run-in behavior of diamond-like carbon friction in humid air.[26] All tracks run for 12000 total cycles and their three-dimensional optical profilometer surface morphologies and two-dimensional sections are shown in Fig. 5. Under the dry condition 5% RH, the wear track of PCD is distract with apparent damage surface comparing that in the higher RH levels environment (10% -50% RH). However, a low friction coefficient is obtained in the dry sliding (5% RH) with a higher loss. Surprisingly but interestingly, almost no wear or rubbing scar is on PCD surfaces tested in higher RH levels (10% -50% RH) conditions, although the friction coefficients are relatively higher than that in dry environments 5% RH. With the increasing of RH levels, the depths of wear track become shallow and wider.

RSC Advances Accepted Manuscript

The wear rates can be calculated from the two-dimensional sections with length of wear tracks (Fig. 6). The tracks created with higher loads and lower relative humidity levels exhibit higher wear rate, and the maxium wear rate is ~ 9×10^{-11} mm^3/Nm.

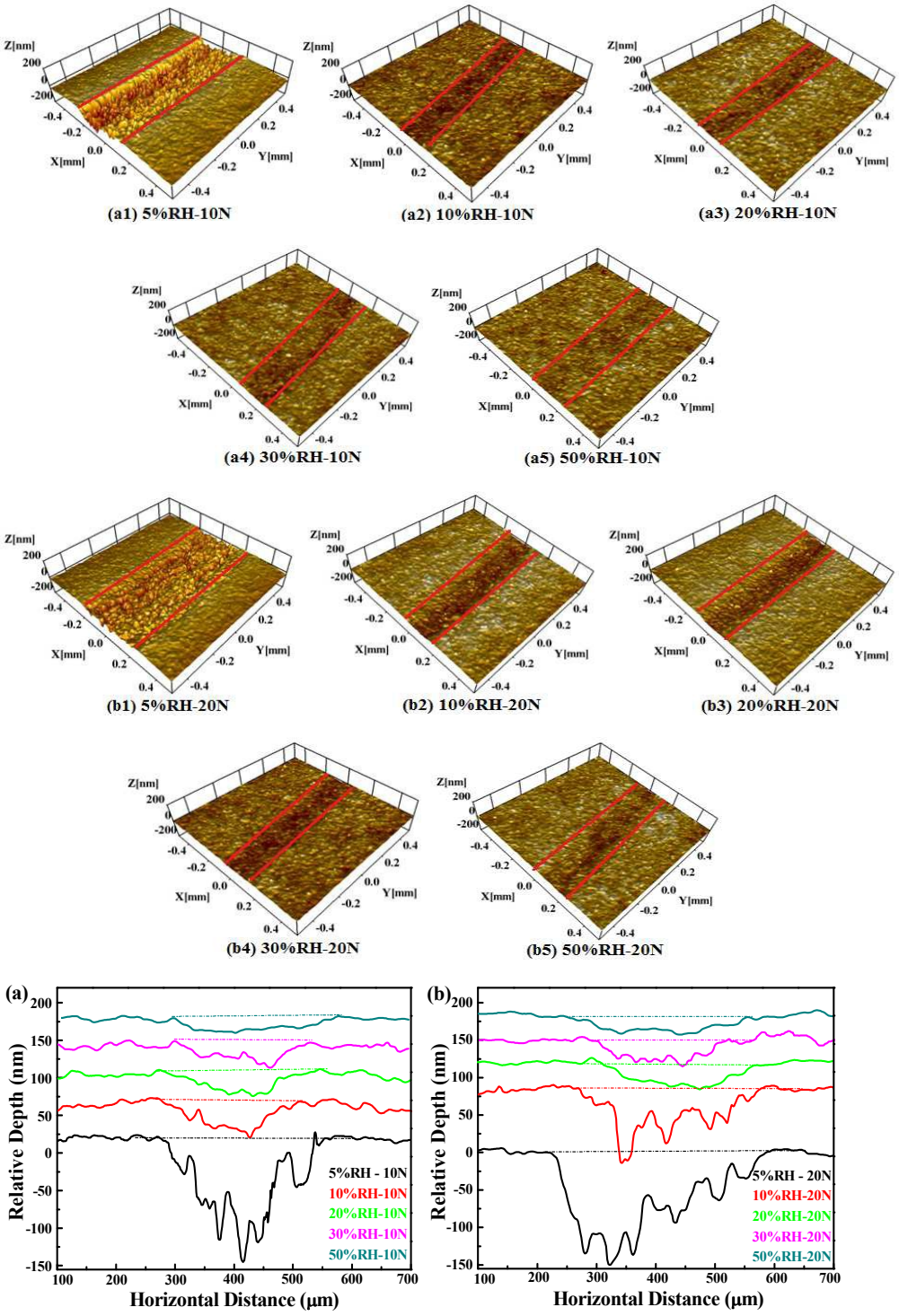

RSC Advances Accepted Manuscript

Fig. 5 Three-dimensional optical profilometer surface morphologies of wear tracks obtained under different RH and loads: a1-a5 wear tracks formed at load of 10 N and b1-b5 at load of 20 N; (a), (b) the two-dimensional cross-sections of wear track. All tracks were run for 12000 total cycles.

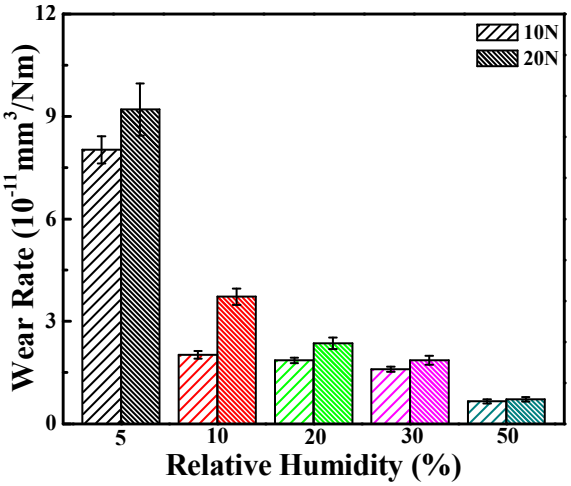

Fig. 6 The comparison of wear rates for PCD wear tracks under various RH levels and loads. Error bars are standard errors and represent variation within a set of measurements.

3.2 Origin of carbonaceous transfer films formation at sliding interface

In order to understand the role of the transfer film in the friction process, Raman spectroscopy was used to investigate the chemical characteristics on the wear scar and track regions.[21,32] Raman intensities of the as-obtained carbonaceous transfer film versus RH levels are displayed in Fig. 7. The magnified view of Raman Shift from 1200-1800 cm^{-1} is shown in Fig. 7b, d. The pairs of peak assigned as D and G bands at 1360 cm^{-1} and 1588 cm^{-1}, respectively, correspond to a-C and sp^2 C=C bonded carbon.[41] An important, but not fully exploited, the D and G features of transfer films are distinctly different from those of the wear tracks. The D-peaks (~1360 cm^{-1}) and G-peaks (~1585 cm^{-1}) evolved from a shoulder to a distinct, high-intensity peak indicats an increasing in cluster size.[42] It means that an evidence that the transfer films contain some carbon rehybridization from

RSC Advances Accepted Manuscript

sp^3 to sp^2 bonding, and microcrystalline graphitic sheets and disorder carbon formation are found on the wear scars of Si_3N_4 spheres. A shift in the G-peak, a high-intensity of the spectrum, may be correlated with the relative amount of transfer film. A stable transfer film growth is observed on the Si_3N_4 sphere under 5% RH (comparing with Fig. 4). Besides, the diverse intensities of D and G peaks are detected on different wear scar locations.[43] Several other peaks with Raman Shift from 300-1200 cm^{-1} observed in the spectra are nearly similar as the chemical characteristics of the virgin Si_3N_4 spheres which is shown in inset Fig. 7e.[44]

Furthermore, Raman spectroscopy measurements of wear tracks on PCD are plotted in Fig. 8. The Raman spectral features such as peak position, intensity and shape on wear tracks of PCD layer are quite different as compared to those obtained from the scar regions of Si_3N_4 spheres. The Raman spectra obtained from the bright white regions only exhibit the characteristic peak of sp^3-bonded diamond (inset Fig. 8d). Whereas, an obvious graphite peak (1580 cm^{-1}) and the disordered graphite peak (1380 cm^{-1}) are detected on the spalling pits regions formed by diamond particles falling off. In the wear track regions, under 5% RH condition, the strong D and G peaks was observed at 1380 cm^{-1} and 1580 cm^{-1} indicate a strong carbon rehybridization. The spectral behaviors in these wear tracks of PCD layer are comparatively similar to the wear scar locations formed on Si_3N_4 spheres, but there are slight changes in peak position, especially the shape and intensity of D and G peaks. A decrease in G band intensity is observed with the increasing of RH levels, indicating sp^2 C-C bonding being weaken. What's more, in all the locations of wear track formed under 10% -50% RH, the Raman spectral characteristics are more or less similar.

RSC Advances Accepted Manuscript

An incisive peak approximately 1332 cm^{-1} is observed corresponding to the existence of sp^3-bonded diamond[45-46] and a particular wear track depicted the intensity of peaks at 1332 cm^{-1} increasing with the RH levels various from 10% to 50%.

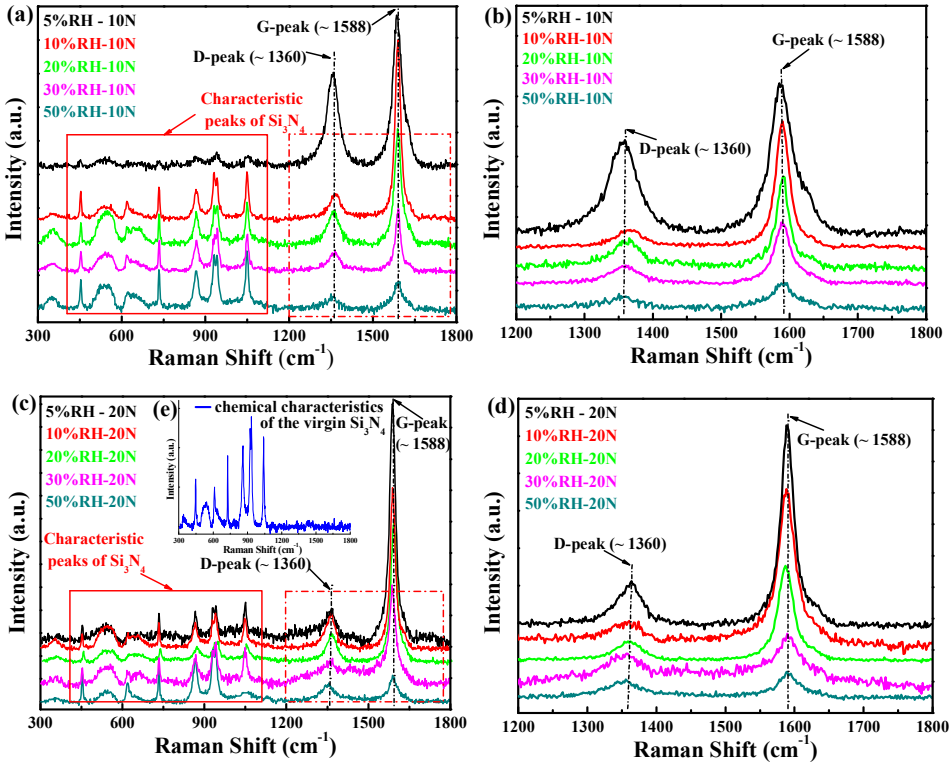

Fig. 7 Raman intensities of transfer film versus RH levels:(a), (c)total peaks displayed with Raman Shift 300-1800cm^{-1}, (b), (d) a magnified view of Raman Shift 1200-1800cm^{-1} from Fig. (a), (c) red gitternetzlinien shown to highlight the C-C bonds formation of transfer film, indicating direct evidence that explains the transfer films formations in highly deformed region of the ball scar. The inset (e) is the Raman spectra of the virgin Si_3N_4 and the detecting positions are indicated in section Fig. 4a2.

RSC Advances Accepted Manuscript

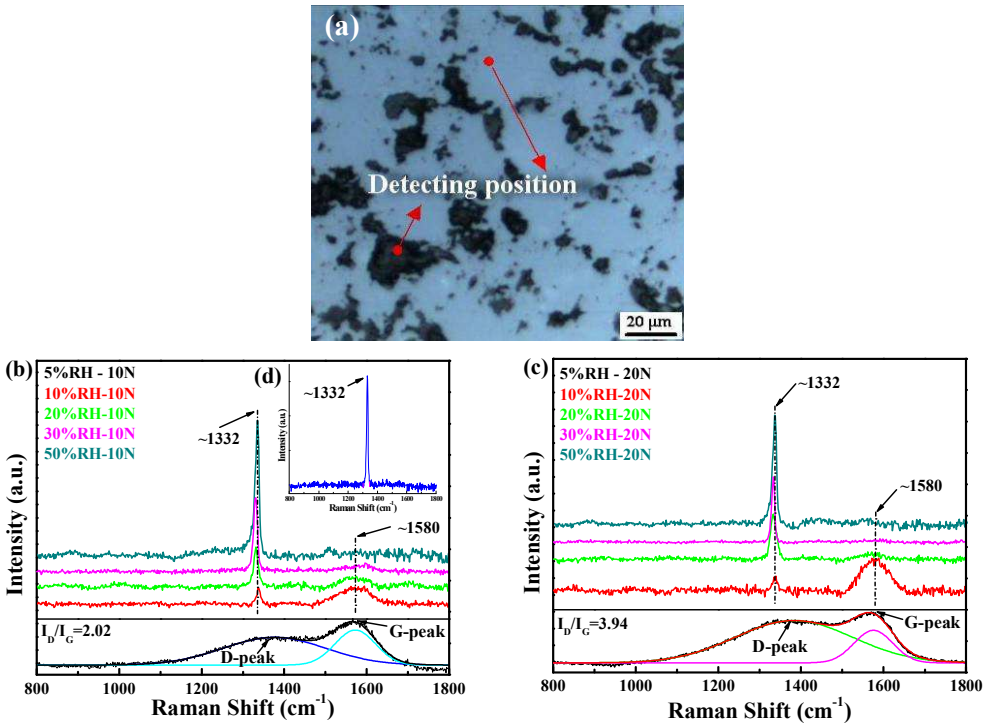

Fig. 8 Raman spectra of wear tracks on PCD surface after friction test under different conditions, (a) showing the detecting position of Raman lase; (b), (c) indicating the carbon bonding states and highlighting the obvious Raman spectrum of D and G peaks taken from the wear tracks under 5% RH both for 10 N and 20 N loads corresponding to the minimum friction coefficient plots displayed in Fig. 3. The inset (d) is the Raman spectra of bright white region.

3.3 Understanding of morphologies build-up and friction force of carbonaceous transfer films in nanoscale measured via an atomic force-force lateral force microscope (AFM-LF)

Atomic force microscopy (AFM) experiments were conducted to test the characteristic morphologies of transfer films and the friction force of transfer film and non-film regions in nanoscale using the lateral force mode. Due to the similar variation tendency of wear scars both for 10 N and 20 N conditions (as shown in Fig. 4), here, AFM experiments get the similar morphologies of transfer films formed at loads 10 N and

RSC Advances Accepted Manuscript

20 N conditions, as shown in Fig. 9a1-a5, 9b1-b5. AFM results further confirm the transfer films formation via Raman spectroscopy analysis. Under low RH especially 5% RH conditions, the transfer films formed on the wear scars are consecutive and homogeneous with the maximum thickness ~ 400 nm (Fig. 9c, d). With the increase of RH levels, the thicknesses of transfer films rapidly decrease. The most obvious phenomena are that no abundant lamellar transfer films is detected and only fragmentary transfer films adhere to the surface of Si_3N_4 sphere scars under higher RH especially 50% RH. The AFM results of transfer films' topographies are essentially in agreement with the optical images of wear scar shown in Fig. 4.

The increased friction forces can be attributed to increased shear strength at contact area. The difference between transfer film and non film regions are displayed in Fig. 9e, f. The friction force test results indicate that friction force values in non-film regions are much higher than that of transfer films regions. The low friction force values of carbonaceous transfer films ensure extremely excellent solid lubrication effects and decrease the shear strength and adhesive interactions across the sliding interfaces of frictional pairs. Therefore, the friction coefficients are intimately correlated with the carbonaceous transfer films on the sliding interfaces.

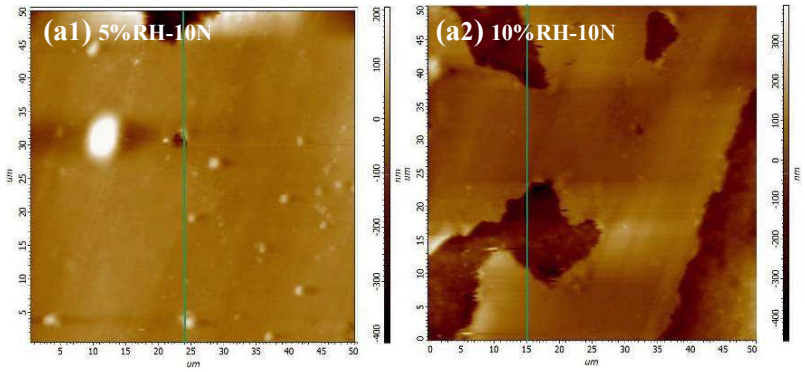

RSC Advances Accepted Manuscript

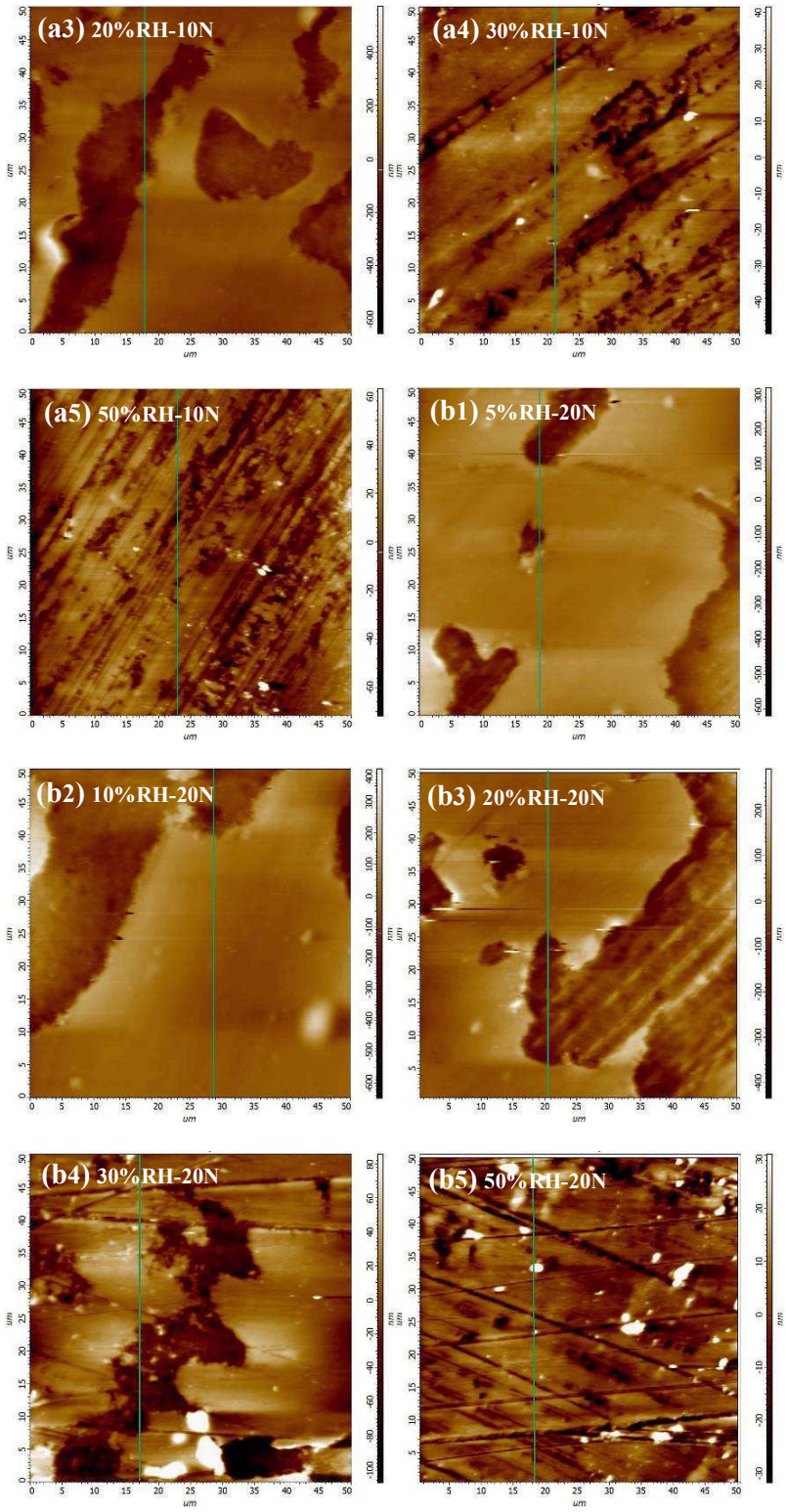

RSC Advances Accepted Manuscript

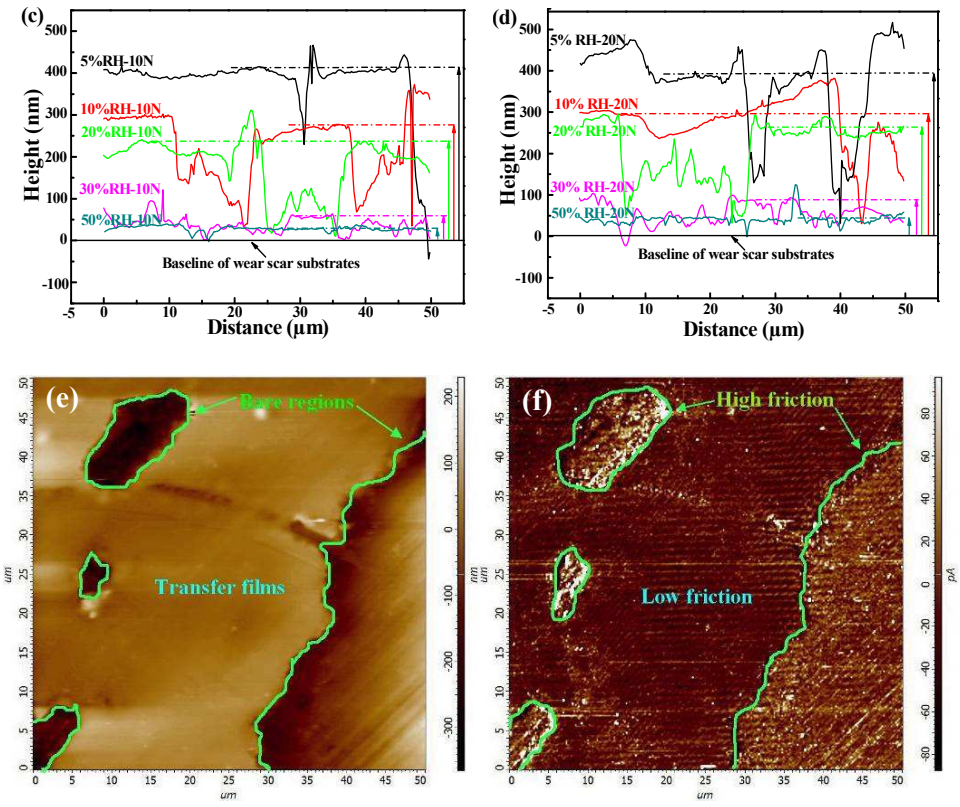

Fig. 9 Atomic force microscopy measurements of transfer films. (a1)-(a5), (b1)-(b5) are the two-dimensional morphologies of transfer films formed at different RH conditions and 10 N, 20 N loads, respectively. (c), (d) are the distribution of thickness corresponding to the green solid lines on Fig. (a1)-(a5) and (b1)-(b5). (e), (f) point out the difference of friction force between film and non-film regions formed at 20 N, 10% RH conditions and the bright green solid depict the non film regions.

4. Discussion

The results demonstrate that the tribological behaviors of PCD matching with Si_3N_4 spheres are strongly controlled by the RH levels in the testing environment and moderately influenced by applied loads, especially the buildup of friction-reduction transfer films at the sliding interface under various RH levels. During the tribotests, the

RSC Advances Accepted Manuscript

rubbing process involves some key issues such as the phase transformation (i.e., sp^3 to sp^2 evolution), running-in period, tribolayer formation, pressure induced bond breaking and formation, passivation with gaseous species or even shear localization in the very thin top interface.[33,47-49] However, during the frictional sliding process, the internal relationship and interaction mechanisms among these factors are complicated.

4.1. Effects of surface and interface adsorbent passivation in the run-in period under different RH level conditions

Experimental elucidation of the role of humidity with dangling bond passivation theory of the H-terminated, OH-terminated surface and the evolution of carbon atoms are complicated by the facts that they can be difficult to isolate the influence of these factors on adhesion and friction.[16,25] The absorbent species affect the adhesive force of the sliding interface, besides the wear performance can be seriously influenced. Barthel et al.[50] studied the effects of gas or vapor adsorption on adhesion, friction, and wear of solid interfaces, and they pointed out that the adsorption of water molecules affect the adhesion, friction, and wear by altering the surface energy of solid interface. The water molecules coming from the moisture ambient atmosphere can adsorbed on the narrow fine draw of the contact interface by forming nanoscale meniscus.[51] Such adsorbed species can raise the forces like hydrogen bonding and capillarity and increase the friction force. These additional forces may be added to the sliding interface and then the adhesion mechanism is changed.[52]

Fig. 10 displayed the contact angle of PCD layer is 65°, indicating PCD surface with a hydrophilic surface.[53] The dangling bonds on the topmost surface of PCD can be

RSC Advances Accepted Manuscript

passivated by forming H-, OH-, H_2O-terminated surface from the dissociation of vapor-phase H_2O absorbed on the sliding interface. The schematic of surface dangling passivation theory is depicted in Fig. 11. Consequently, the formation of H-, OH-, and H_2O-terminated surface can saturate the carbon dangling bonds with the decreasing of interface energies. The saturated carbon bonds can prevent the covalent bonds generating in the interface, and the friction force between PCD and Si_3N_4 spheres decreased. However, under dry atmospheres ~ 5% RH, the dangling bonds of PCD and Si_3N_4 spheres surface can not be effectively passivated, which results in strong interaction by forming covalent between sliding interface. The strong covalent interaction results in the increasing of initial friction force corresponding to the longer run-in period under 5% RH conditions. Besides, this un-terminated surface may be quickly grinded off with higher wear rate (as shown in Fig. 6). With the increasing of RH levels (from 10% to 50% RH), the un-saturated carbon dangling bonds can be adequately passivated with enough water molecules. If the new dangling bonds form, the high concentration water molecules can shorten the time of re-passivated, and then the dangling bonds can be promptly re-passivated. Therefore, the higher RH levels corresponding to the shorter run-in periods and lower wear rates of PCD. However, the insufficient transfer films formed on the spheres result in that the wear of Si_3N_4 spheres increase with the variation of RH levels from 10% to 50% for both 10 N and 20 N. Due to the strong covalent interaction between PCD un-terminated surfaces and Si_3N_4 spheres at 5% RH condition, a higher wear scar is still formed. At high RH levels condition, the Si_3N_4 is easier to react with H_2O by forming SiO_2 [54] and then its wear is more serious than that in lower RH levels. However, due to the

RSC Advances Accepted Manuscript

strong dangling bonds passivation by forming H-, OH-, and H_2O-terminated surface under high RH condition, less surface unsaturated atoms can form covalent interaction across the sliding interface. Consequently the wear loss of PCD decreases with the increase of RH levels.

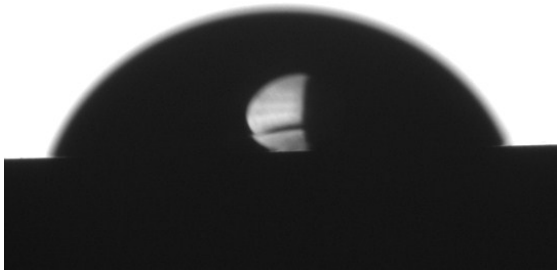

Fig. 10 Typical water contact angle measuring image of PCD layers, indicating a hydrophilic surface of PCD layer (with water contact angle 65°).

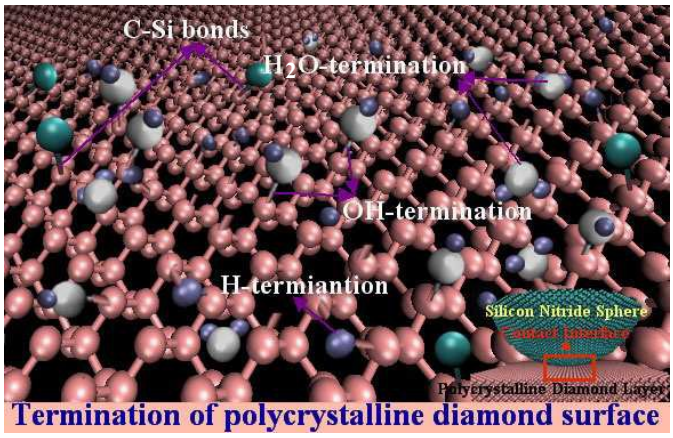

Fig. 11 Schematic with ball-and-stick representations of the surface dangling bonds passivation via forming H-terminated, OH-terminated, H_2O-terminated surface. (a) Far view of inset shows contact geometry. (b) Close view of polycrystalline diamond surface. Solid rotundity ice blue, off-white, red and blue-green represent Hydrogen, Oxygen, Carbon, and Nitrogen atom, respectively.

4.2 Overview of the formation of transfer film in different run-in periods

Running-in period is a key factor controlling the tribological performances in a-C films.[55] Firstly, in the process of dry sliding, a transfer film (a carbon rich layer with high

RSC Advances Accepted Manuscript

sp^2 content) will be generated in the small contact region of Si_3N_4 spheres, which will prevent stiff ball from contacting the hard film directly and decrease the shear strength and adhesion at the sliding interface. The transfer film is generated by destroying the surface layer of film at the run-in period of tribological test.

The formation of carbonaceous transfer films on the wear scars is quite significant as observed in Raman spectra (Fig. 7). It is shown that the formations and breaks of covalent bonds during sliding result in the development of transfer films. In such a condition, the tribolocical testing evolves into sliding between Si_3N_4 spheres and carbonaceous transfer films.

Under dry testing atmosphere with low RH level ~5% RH corresponding to the maximum run-in period ~ 4000 cycles, an insufficient concentration of water molecules distribution in tribometer chamber result in a deficiency surface passivation of PCD surfaces with unterminated carbon. These unsaturated carbon atoms serve as initiation points for the formation of covalent bonds between the counterface and the PCD surface, which can consequently bring strong adhesive interactions. These adhesive interactions cause an increase in friction force during the initial sliding corresponding to the run-in period anomalously high friction coefficient seen in the first 2000 and 4000 cycles (Fig. 3b, d). However, the formation and breaking of covalent bonds during sliding with strong interactions by forming C-Si bonds at interface results in the formation of a transfer film (a carbon rich layer with high *sp*^{2} content). Soon afterwards, an ultralow steady-state friction coefficient created, indicating the formation of transfer film can decrease the adhesive interactions between the PCD surface and the counterface by protecting the PCD

RSC Advances Accepted Manuscript

surface from directly contacting with matching sphere (displayed in the Fig. 9). As abovementioned, the transfer film cannot be generated effectively in time under higher RH levels (10%-50%) corresponding to the inconspicuous run-in periods, which results in higher friction without transfer films effective protection at the interface. What's more, Schall *et al*.[16] have reported the effects of adhesion and transfer films formation on the tribology of self-mated DLC contacts using molecular dynamics simulations, when covalent bonds break, friction decreases and there is a concomitant increase in the local temperature emanating from the interface. When the temperature of the sliding real contact area is higher than the graphitization temperature, the formation of graphite being relate to the transfer film between the sliding interfaces can decrease the friction coefficient as an exceptional solid lubrication. Fig. 12 is the diagrammatic drawing of transfer films formations at the sliding interface, indicating that transfer layers prevent PCD surface immediately contacting with Si_3N_4 sphere. Therefore, the efficient transfer films formed during the longer run-in period can ensure the frictional system achieve a minimum steady-state friction coefficient. In order to further confirm the transfer films formation and wear occur in run-in period, we conducted another run-in tribotest at 20 N and 5% RH conditions. This tribotest was intentionally terminated after run-in period ~ 2000 cycles and then compare the difference of wear scar with that formed at the total sliding cycles. Fig. 13 displays the variation of wear scar formed at different sliding cycles. The wear scar formed at the run-in period are similar to those formed at the total sliding cycles. It strongly demonstrate that the transfer film formation mainly occur in run-in period and that can be suppressed by dangling bonds passivation effects.

RSC Advances Accepted Manuscript

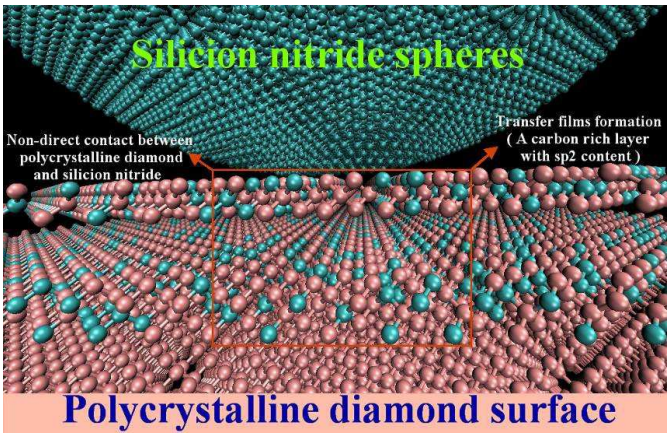

Fig. 12 Schematic description of contact between Si_3N_4 sphere, transfer film and PCD, the red box correspond to transfer films.

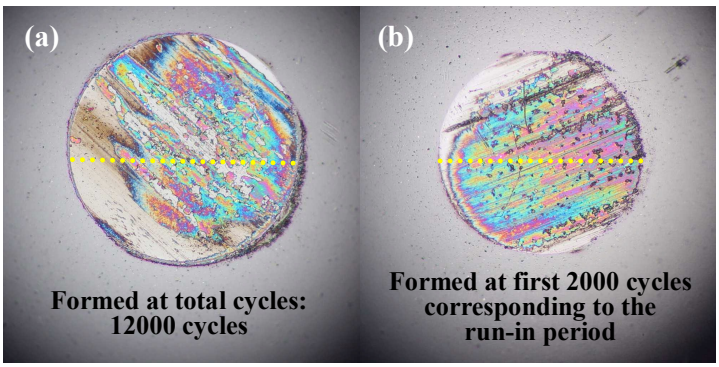

Fig. 13 Comparison of wear scars formed at 5%RH, 20 N with different sliding cycles: (a) the total cycles, (b) the first 2000 cycles. This comparison to strongly highlight the transfer films formed at the run-in periods.

4.3 Understanding in competitive effects of transfer films formation and surface dangling bonds passivation

Fig. 14 shows the relationships among RH levels, thickness and steady-state friction coefficient. With the increasing of RH levels, the thicknesses of transfer film decrease and it result in the increase of the steady-state friction coefficient. Thus, the obvious relationship and the leading factor of influencing tribological behaviors must be understood systematically. We can concluded that the interaction relationships between

RSC Advances Accepted Manuscript

surface dangling bonds passivation and transfer films formation are complicated based on the above analysis. Under dry atmosphere ~ 5% RH, due to the extreme low concentration water molecules, the dangling bonds passivation effect is inconspicuous. The tribological systems keep a longer run-in period ~ 4000 cycles before reaching ultra-low steady-state friction coefficient ~ 0.04. With the increasing of RH levels, surface dangling bonds passivation play the leading role in the chemical action across interface during the run-in period. Previously, experimental elucidation of the role of humidity with dangling bond passivation theory of forming the H-terminated, OH-terminated surface have been reported. [11,23-24] Such saturated carbon bonds can not form covalent networking in the counterface and decrease the adhesive interactions resulting in an decrease in friction,[50,56] which can be with a briefer run-in period corresponding to the inefficient transfer films formation resulting in the increase of friction coefficient abovementioned. Therefore, the RH levels influence the dangling bonds passivation effect, and then the dangling bonds passivation effects can strongly affect the covalent interaction at the sliding interface corresponding to the length of run-in period. Finally, the longer run-in period assure the transfer film effectually formed. The real factor of behaving low steady-state friction coefficient is the efficient and continuous transfer films formation.

Based on the current works of this paper, under different RH levels atmosphere, the effects of transfer films formation on the decreasing of the steady-state friction coefficient of PCD have been discovered and the relationships among RH levels, run-in periods, and steady-state friction coefficient and transfer films formation have been discussed in details hereinbefore. For further interpretation and demonstration how the adsorption of water

RSC Advances Accepted Manuscript

molecules affect the sliding interface tribochemical reactions and indirectly influence the formation of transfer films are still insufficient, which is a key theoretical issue of concern in drilling engineering. For the next step of works, the characterization of the effects of interfacial tribochemical reactions on the transfer films formation would be systematically explored. However, the understanding of integrated effects of humidity and interfacial transfer films formation on tribological behaviors of sintered PCD materials is very meaningful for reasonably designing the lubricating system when PCD as down-hole applications used in the drilling exploitation field.

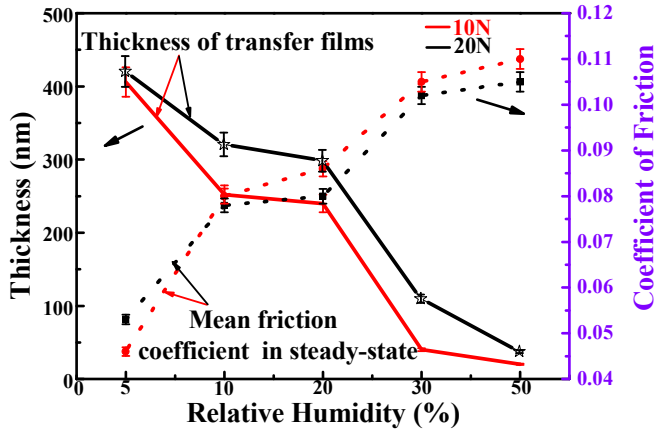

Fig. 14 Comparison between transfer films' thicknesses and mean fiction coefficient in steady-state as a function of RH levels. Solid black and red lines show the variation of transfer films. Dotted black and red lines show the variation of mean friction coefficient. Error bars are standard errors and represent variation within a set of measurements.

5. Conclusions

This work presented the tribological behaviors of PCD layers sliding against Si_3N_4 spheres in various loads and RH levels. An overarching conclusion is that carbonaceous transfer film formation is affected by RH levels and the overall tribological behaviors are

RSC Advances Accepted Manuscript

controlled by the competition interaction between dangling bonds passivation and transfer film formation.

As a result, ultra-low steady-state friction coefficient ~ 0.04, ~ 0.06 and corresponding to higher wear rate ~ 8×10^{-11} mm^3/Nm, ~ 9.1×10^{-11} mm^3/Nm were observed under 5% RH condition. The run-in period and wear rate of PCD rapidly decrease while increasing RH levels during the tribotest. Such ultra-low steady-state friction coefficient is predominantly governed by the carbonaceous transfer films formation on the Si_3N_4 spheres which are closely correlated with the cycles of reaching run-in period. This carbonaceous transfer films can significantly decrease the adhesive interactions at the counterface by protecting the PCD surface from directly contacting with counter spheres. Furthermore, from the optical images of wear scars formed on Si_3N_4 spheres, we can summarize that the diameters of wear scars increase with the variation of RH levels from 10% to 50% both for 10 N and 20 N. Due to the strong covalent interaction between PCD un-terminated surfaces, a higher wear scar of Si_3N_4 spheres was still formed at 5% RH condition.

In conclusion, the results demonstrate that the RH levels influence the dangling bonds passivation effect. Furthermore, the dangling bonds passivation effects affect the covalent interaction at the sliding interface corresponding to the length of run-in period and the wear rates of PCD surface. Finally, the longer run-in period and higher wear loss of PCD assure the transfer film effectually form, and the real factor of showing low steady-state friction coefficient is the efficient and continuous transfer films formation.

RSC Advances Accepted Manuscript

Acknowledgements

We acknowledge the National Natural Science Foundation of China (51375466) and the International Science and Technology Cooperation Project of China (2011DFR50060) for the financial support.

Notes and references

1. B. A. Lingwall, T. N. Sexton and C. H. Cooley, *Wear*., 2013, **302**, 1514–1519.

2. D. R. Hall, *U.S. Patent*., 1986, **106**, 604.

3. R. M. Erasmus, J. D. Comins, V. Mofokeng and Z. Martin, *Diamond Relat. Mater*., 2011, **20**, 907–911.

4. M. K. Keshavan, B. Liang and M. Russel, *Smith International, Inc*., 1989.

5. M. W. Cook, *Ind. Diamond Rev*., 1996, **56**, 107–111.

6. T. N. Sexton and C. H. Cooley, *Wear*., 2009, **267**, 1041–1045.

7. C. W. Knuteson, T. N. Sexton and C. H. Cooley, *Wear*., 2011, **271**, 2106–2110.

8. R. L. Mehan and L. E. Hibbs, *J. Mater. Sci*., 1989, **24**, 942–950.

9. K. Enke, H. Dimigen and H. Hübsch, *Appl. Phys. Lett*., 1980, **36**, 291–292.

10. M. J. Marino, E. Hsiao, Y. Chen, O. L. Eryilmaz, A. Erdemir and S. H. Kim, *Langmuir*., 2011, **27**, 12702–12708.

11. A. R. Konicek, D. S. Grierson, A. V. Sumant, T.A. Friedmann, J. P. Sullivan, P. U. P. A. Gilbert, W. G. Sawyer and R. W. Carpick, *Phys. Rev. B*., 2012, **85**, 155448.

12. N. Kumar, Radhika Ramadoss, A. T. Kozakov, K. J. Sankaran, S. Dash, A. K. Tyagi, N. H. Tai and I-. Nan Lin, *J. Phys. D: Appl. Phys*., 2013, **46**, 275501.

13. Y. Zhao, W. Yue, F. Lin, C. Wang and Z. Wu, *Int. J. Refract. Met. Hard Mater*., 2015, **50**, 43–52.

RSC Advances Accepted Manuscript

14. A. P. Merkle, A. Erdemir, O. L. Eryilmaz, J. A. Johnson and L. D. Marks, *Carbon*., 2010, **48**, 587–591.

15. H. Liu, A. Tanaka and T. Kumagai, *Thin Solid Films*., 1999, **352**, 145–150.

16. J. D. Schall, G. Gao and J. A. Harrison, *J. Phys. Chem. C*., 2009, **114**, 5321–5330.

17. J. C. Sanchez-Lopez, A. Erdemir, C. Donnet and T. C. Rojas, *Surf. Coat. Technol*., 2003, **163**, 444–450.

18. Y. Liu, A. Erdemir and E. I. Meletis, *Surf. Coat. Technol*., 1996, **86**, 564–568.

19. U. Bögli, A. Blatter, S. M. Pimenov, E. D. Obraztsova, A. A. Smolin, M. Maillat and E. N. Loubnin, *Diamond Relat. Mater*., 1995, **4**, 1009–1019.

20. X. Chen, T. Kato and M. Nosaka, *ACS. Appl. Mater. Interfaces*., 2014, **6**, 13389–13405.

21. R. Radhika, N. Kumar, A. T. Kozakov, K. J. Sankaran, S. Dash, A. K. Tyagi and I. N. Lin, *Diamond Relat. Mater*., 2014, **48**, 6–18.

22. A. A. Voevodin, J. P. O'neill and J. S. Zabinski, *Thin Solid Films*., 1999, **342**, 194–200.

23. P. A. Romero, L. Pastewka, J. Von Lautz and M. Moseler, *Friction*., 2014, **2**, 193–208.

24. L. Cui, Z. Lu and L. Wang, *ACS. Appl. Mater. Interfaces*., 2013, **5**, 5889−5893.

25. A. R. Konicek, D. S. Grierson, P. U. P. A. Gilbert, W. G. Sawyer, A. V. Sumant and R. W. Carpick, *Phys. Rev. Lett*., 2008, **100**, 235502.

26. S. Bai, H. Murabayashi, Y. Kobayashi, Y. Higuchi, N. Ozawa, K. Adachi, J. M. Martin and M. Kubo, *RSC Adv*., 2014, 4, 33739−33748.

27. L. Ji, H. Li, F. Zhao, W. Quan, J. Chen and H. Zhou, *J. Phys. D: Appl. Phys*., 2009, **42**, 135301.

28. Z. Chai, Y. Liu, X. Lu and D. He, *RSC Adv*., 2014, **4**, 51047–51054.

29. D. Tabor, *Tribol. Lett*., 1981, **368**.

RSC Advances Accepted Manuscript

30. D. I. Kim, J. Grobelny, N. Pradeep and R. F. Cook, *Langmuir*., 2008, **24**, 1873–1877.

31. A. C. Ferrari, J. *Phys. Rev. B*., 2001, **64**, 075414.

32. T. W. Scharf and I. L. Singer, *Tribol. Lett*., 2003, **14**, 3–8.

33. R. R. Chromik, A. L. Winfrey, J. Lüning, R. J. Nemanich and K. J. Wahl, *Wear*., 2008, **265**, 477–489.

34. L. Pastewka, S. Moser, P. Gumbsch and M. Moseler, *Nat. Mater*., 2011, **10**, 34–38.

35. O. J. Furlong, B. Miller, P. V. Kotvis, H. L. Adams, W. T. Tysoe, *RSC Adv*., 2014, **4**, 24059−24066.

36. G. Amontons, *Mem. Acad. R. A*., 1699, **12**, 275–282.

37. S. G. Moseley, K. P. Bohn and M. Goedickemeier, *Int. J. Refract. Met. Hard Mater*., 2009, **27**, 394–402.

38. M. Godet, *Wear*., 1984, **100**, 437–452.

39. S. E. Grillo and J. E. Field, *Phys. D: Appl. Phys*., 1997, **30**, 202.

40. Y. Mo, K. T. Turner and I. Szlufarska, *Nature*., 2009, **457**, 1116–1119.

41. R. M. Erasmus, J. D. Comins, V. Mofokeng and Z. Martin, *Mater*., 2011, **20**, 907–911.

42. R. Haubner and M. Rudigier, *Physics Procedia*., 2013, **46**, 71–78.

43. M. Veres, S. Tóth, Á. Kukovecz and M. Koós, *Diamond Relat. Mater*., 2008, **17**, 515–519.

44. M. Chen, K. Kato and K. Adachi, *Tribol. Lett*., 2002, **35**, 129–135.

45. D. S. Knight and W. B. White, *J. Mater. Res*., 1989, **4**, 385–393.

46. X. Yu, X. Zhao, Y. Liu, M. Hua and X. Jiang, *ACS. Appl. Mater. Interfaces*., 2014, **6**, 4669–4677.

47. S. Ohnishi and A. M. Stewart, *Langmuir*., 2002, **18**, 6140–6146.

48. M. I. De Barros Bouchet, G. Zilibotti, C. Matta, M. C. Righi, L. Vandenbulcke, B. Vacher and J. M. Martin, *J. Phys. Chem. C*., 2012, **116**, 6966–6972.

RSC Advances Accepted Manuscript

49. F. Wang, W. Wu, J. Li, S. Li, Y. Tang and W. Sun, *Sci. China, Ser. E*., 2009, **52**, 850–856.

50. A. J. Barthel, A. Al-Azizi, N. D. Surdyka and S. H. Kim, *Langmuir*., 2013, **30**, 2977–2992.

51. A. A. Feiler, J. Stiernstedt, K. Theander, P. Jenkins and M. W. Rutland, *Langmuir*., 2007, **23**, 517–522.

52. D. L. Sedin and K. L. Rowlen, *Anal. Chem*., 2000, **72**, 2183–2189.

53. S. Liu, G. Xie, D. Guo and Y. Liu, *J. Appl. Phys*., 2010, **107**, 104323.

54. M. Chen, K. Kato, K. Adachi, *Wear*., 2001, **250**, 246–255.

55. X. Chen, T. Kato, M. Kawaguchi and J. Choi, *J. Phys. D: Appl. Phys*., 2013, **46**, 255304.

56. J. -M. Martin, M. -I. De Barros Bouchet, C. Matta, Q. Zhang, W. A. Goddard, III S. Okuda and T. Sagawa, *J. Phys. Chem. C*., 2010, **114**, 5003−5011.

RSC Advances Accepted Manuscript